RESEARCH ARTICLE

Association with PAK2 Enables Functional Interactions of Lentiviral Nef Proteins with the Exocyst Complex

Andrea Imle,[a] Libin Abraham,[a]* Nikolaos Tsopoulidis,[a] Bernard Hoflack,[b] Kalle Saksela,[c] Oliver T. Fackler[a]

Department of Infectious Diseases, Integrative Virology, University Hospital Heidelberg, Heidelberg, Germany[a]; Biotechnological Center, Technische Universität Dresden, Dresden, Germany[b]; Department of Virology, University of Helsinki and Helsinki University Hospital, Helsinki, Finland[c]

* Present address: Libin Abraham, Department of Microbiology & Immunology, University of British Columbia, Vancouver, British Columbia, Canada.

ABSTRACT **Human immunodeficiency virus type 1 (HIV-1) Nef enhances virus replication and contributes to immune evasion *in vivo*, but the underlying molecular mechanisms remain incompletely defined. Nef interferes with host cell actin dynamics to restrict T lymphocyte responses to chemokine stimulation and T cell receptor engagement. This relies on the assembly of a labile multiprotein complex including the host kinase PAK2 that Nef usurps to phosphorylate and inactivate the actin-severing factor cofilin. Components of the exocyst complex (EXOC), an octameric protein complex involved in vesicular transport and actin remodeling, were recently reported to interact with Nef via the same molecular surface that mediates PAK2 association. Exploring the functional relevance of EXOC in Nef-PAK2 complex assembly/function, we found Nef-EXOC interactions to be specifically mediated by the PAK2 interface of Nef, to occur in infected human T lymphocytes, and to be conserved among lentiviral Nef proteins. In turn, EXOC was dispensable for direct downstream effector functions of Nef-associated PAK2. Surprisingly, PAK2 was essential for Nef-EXOC association, which required a functional Rac1/Cdc42 binding site but not the catalytic activity of PAK2. EXOC was dispensable for Nef functions in vesicular transport but critical for inhibition of actin remodeling and proximal signaling upon T cell receptor engagement. Thus, Nef exploits PAK2 in a stepwise mechanism in which its kinase activity cooperates with an adaptor function for EXOC to inhibit host cell actin dynamics.**

IMPORTANCE **Human immunodeficiency virus type 1 (HIV-1) Nef contributes to AIDS pathogenesis, but the underlying molecular mechanisms remain incompletely understood. An important aspect of Nef function is to facilitate virus replication by disrupting T lymphocyte actin dynamics in response to stimulation via its association with the host cell kinase PAK2. We report here that the molecular surface of Nef for PAK2 association also mediates interaction of Nef with EXOC and establish that PAK2 provides an essential adaptor function for the subsequent formation of Nef-EXOC complexes. PAK2 and EXOC specifically cooperate in the inhibition of actin dynamics and proximal signaling induced by T cell receptor engagement by Nef. These results establish EXOC as a functionally relevant Nef interaction partner, emphasize the suitability of the PAK2 interaction surface for future therapeutic interference with Nef function, and show that such strategies need to target activity-independent PAK2 functions.**

Received 31 July 2015 **Accepted** 5 August 2015 **Published** 8 September 2015

Citation Imle A, Abraham L, Tsopoulidis N, Hoflack B, Saksela K, Fackler OT. 2015. Association with PAK2 enables functional interactions of lentiviral Nef proteins with the exocyst complex. mBio 6(5):e01309-15. doi:10.1128/mBio.01309-15.

Invited Editor Thomas E. Smithgall, University of Pittsburgh School of Medicine **Editor** Vinayaka R. Prasad, Albert Einstein College of Medicine

Address correspondence to Oliver T. Fackler, oliver.fackler@med.uni-heidelberg.de.

The efficacy with which human immunodeficiency virus type 1 (HIV-1) replicates in the infected host is governed by a complex set of parameters, including the intrinsic replication capacity of the specific virus strain, the potency of the host immune system, and the ability of the virus to evade immune recognition. The so-called accessory genes (*vif*, *vpu*, *vpr*, and *nef*) play important roles in optimizing HIV-1 spread *in vivo* while, depending on the culture conditions used, they can be dispensable for virus replication *ex vivo*. The Nef protein exerts pronounced effects on *in vivo* virus replication and pathogenicity, yet the relevant molecular mechanisms of action remain little defined.

Nef is a myristoylated 25- to 34-kDa protein encoded by HIV-1, HIV-2, and simian immunodeficiency virus (SIV). While entirely dispensable for virus replication in cultured cells, Nef potently increases virus replication and thus serves as a pathogenicity factor that accelerates disease progression in the infected host (1–3). This role of Nef in AIDS pathogenesis is also supported by a transgenic-mouse model in which expression of Nef induces AIDS-like depletion of $CD4^+$ T lymphocytes (4, 5). It is generally assumed that Nef has no enzymatic activity but rather mediates its functions through a large set of interactions with cellular proteins. By virtue of this adaptor function, Nef affects many central processes in HIV target cells. This includes modulation of cellular transport pathways leading to the downregulation of an array of receptors from the surface of infected cells, which, e.g., prevents superinfection (6, 7) and lysis of productively infected cells by cytotoxic T or NK cells (8–10). Nef also enhances HIV-1 particle infectivity (11–14). Finally, HIV-1 Nef alters the response of CD4

T lymphocytes to stimulation via the T cell receptor (TCR), and modulation of the resulting cellular signaling pathways is thought to increase virus replication in the infected host (15–20). One mechanism by which Nef alters TCR signaling is retargeting of active pools of the Src family kinase Lck from the plasma membrane to recycling endosomes and the trans-Golgi network (TGN) (16, 19, 21–25). This compartmentalization of T-cell receptor (TCR) signaling modifies the response of infected T lymphocytes to stimulation by blocking proximal TCR signaling at the plasma membrane and simultaneously triggering a signaling cascade initiated at intracellular membranes (16, 19, 26, 27).

In addition to these alterations of host cell vesicular transport, some of Nef's activities are mediated by its ability to reduce host cell actin remodeling (28–32). Such reduced actin remodeling restricts the ability of T lymphocytes to undergo morphological changes triggered by extracellular stimuli such as TCR engagement and limits their motility toward chemoattractants (23, 29, 31, 33–35). While the physiological consequences of these effects still remain to be elucidated, impaired T lymphocyte motility and cell-cell communication in lymph nodes of infected individuals may favor virus spread and limit the mounting of humoral immune responses (36).

The identification of which molecular interactions of Nef contribute to its role in HIV pathogenesis has been hampered by the large number and low affinity of the ligands identified, as well as by the fact that multiple interaction partners were identified for most of Nef's protein interaction motifs (37–39). Interference with host cell actin remodeling has been an exception in this regard, as it strictly depends on a hydrophobic patch not involved in any other Nef activity reported to date (31, 40–42). Via this patch, Nef associates with a highly active subpopulation of the host cell kinase PAK2 (43, 44) and Nef increases overall PAK2 activity in some cell systems (45). In the case of a HIV-1 clade B Nef such as SF2 or NL4.3, this binding pocket includes a critical phenylalanine (F195 in the case of Nef from HIV-1 SF2), mutations of which specifically disrupt PAK2 association. Association with Nef alters the specificity of PAK2 and results in phosphorylation and thus inactivation of the actin-severing factor cofilin to reduce actin remodeling and thus motility (31, 35, 46). These Nef effects on host cell actin dynamics may also involve additional PAK2-dependent mechanisms and substrates. Nef-PAK2 association occurs in detergent-resistant membrane microdomains (47, 48) and within a larger macromolecular complex (49). Nef-PAK2 complexes are very unstable, and while Nef-associated PAK2 activity can readily be demonstrated by *in vitro* kinase assay (IVKA), detection of Nef-associated PAK2 protein by less sensitive methods such as Western blotting is difficult (43, 44, 49). The full composition of the Nef-PAK2 complex remains to be determined; however, the PAK2-activating small GTPases Cdc42/Rac1, as well as their guanine exchange factor Vav1, were identified as relevant complex components (28, 50–52).

More recent work identified the exocyst complex (EXOC) as a novel cellular ligand of the Nef proteins of HIV-1 NL4-3 (subtype B) and 5C (subtype C) (53, 54). EXOC is an evolutionarily conserved octameric complex thought to tether post-Golgi vesicles to the plasma membrane during polarized secretion. In addition, EXOC has been implicated in the regulation of cell motility by mechanisms that are not linked to its role in exocytosis. Multiple interactions with cytoskeletal players (such as the small GTPases Cdc42 and Ral or the actin nucleator Arp2/3) position EXOC at the interface between vesicle trafficking and polarized cytoskeletal regulation (55–61).

On the basis of silencing experiments, Mukerji et al. suggested EXOC as a mediator of Nef's ability to promote the formation of filopodium-like cell protrusions or nanotubes (53). However, nanotube induction by Nef is a rare event (29, 35) and EXOC is a core component critical for their formation (62). The functional relevance of the Nef-EXOC interaction thus remains to be determined. Importantly, the interaction with EXOC required residues also mediating Nef-PAK2 association (53). This finding challenged for the first time the specificity of these residues for Nef-PAK2 association and suggested that (i) Nef may independently associate with PAK2 and EXOC via these residues or (ii) association of the viral protein with PAK2 and EXOC is coordinated. We therefore set out to investigate the functional relevance of the Nef-EXOC interaction and its relationship to PAK2 association.

RESULTS

Interactions with EXOC via PAK2 association motifs occur in HIV-infected T lymphocytes and are conserved among lentiviral Nef proteins. In a first set of experiments, we tested whether we could detect the association of HIV-1 Nef with EXOC as described by Mukerji et al. (53). To this end, we transfected Jurkat T lymphocytes with expression plasmids for green fluorescent protein (GFP), HIV-1 SF2 Nef fused with GFP (Nef.GFP), or Nef.GFP mutant proteins and immunoisolated these proteins with GFP-Trap beads (Fig. 1A). EXOC subunit 2 (EXOC2) was readily detected in Nef.GFP but not GFP immunoprecipitates. Consistently, mass spectrometry identified all eight EXOC subunits as specifically enriched when liposomes that carried myristoylated Nef were incubated with cell lysate and subsequently isolated by membrane flotation to identify host cell interaction partners of membrane-associated Nef (63; data not shown). Analyses to probe for the presence of Nef.GFP in anti-EXOC immunoprecipitations were hampered by the lack of antibodies that immunoisolate endogenous EXOC subunits without compromising EXOC integrity and the instability of overexpressed epitope-tagged EXOC subunits (data not shown; 64). Mukerji et al. reported that the interaction of 5C Nef, a hyperactive Nef variant with regard to association with PAK2 activity (40), with EXOC required PAK2-interacting residues (53). PAK2-interacting surfaces are, in principle, conserved among lentiviral Nef proteins, although their specific amino acid architecture varies and, as, e.g., in 5C Nef, often does not contain a phenylalanine (see Fig. S1A in the supplemental material). In the case of SF2 Nef, the Nef-PAK2 association is disrupted by the F195A mutation or mutation of the proline-rich SH3 domain binding motif (mutant Nef protein AxxA) (38). These mutations strongly reduced Nef's association with EXOC2 (Fig. 1A to C, 23.2% ± 17.0% for F195A and 11.9% ± 9.5% for AxxA, i.e., percentage of coimmunoprecipitated EXOC2 of immunoprecipitated GFP expressed relative to that of wild-type [WT] SF2, which was set to 100%). More extensive screening of a panel of well-characterized mutant Nef proteins (Fig. 1B and C) revealed that a mutant Nef protein with a disruption of the acidic stretch mediating interaction with the sorting adaptors PACS/AP-1 (E4A4) (65–67) also displayed only residual interaction with EXOC in most of our experiments (19.3% ± 12.5%; see Fig. S2 in the supplemental material for a single experiment in which the interaction was enhanced). This acidic stretch thus represents an additional determinant in Nef for EXOC interaction that is also

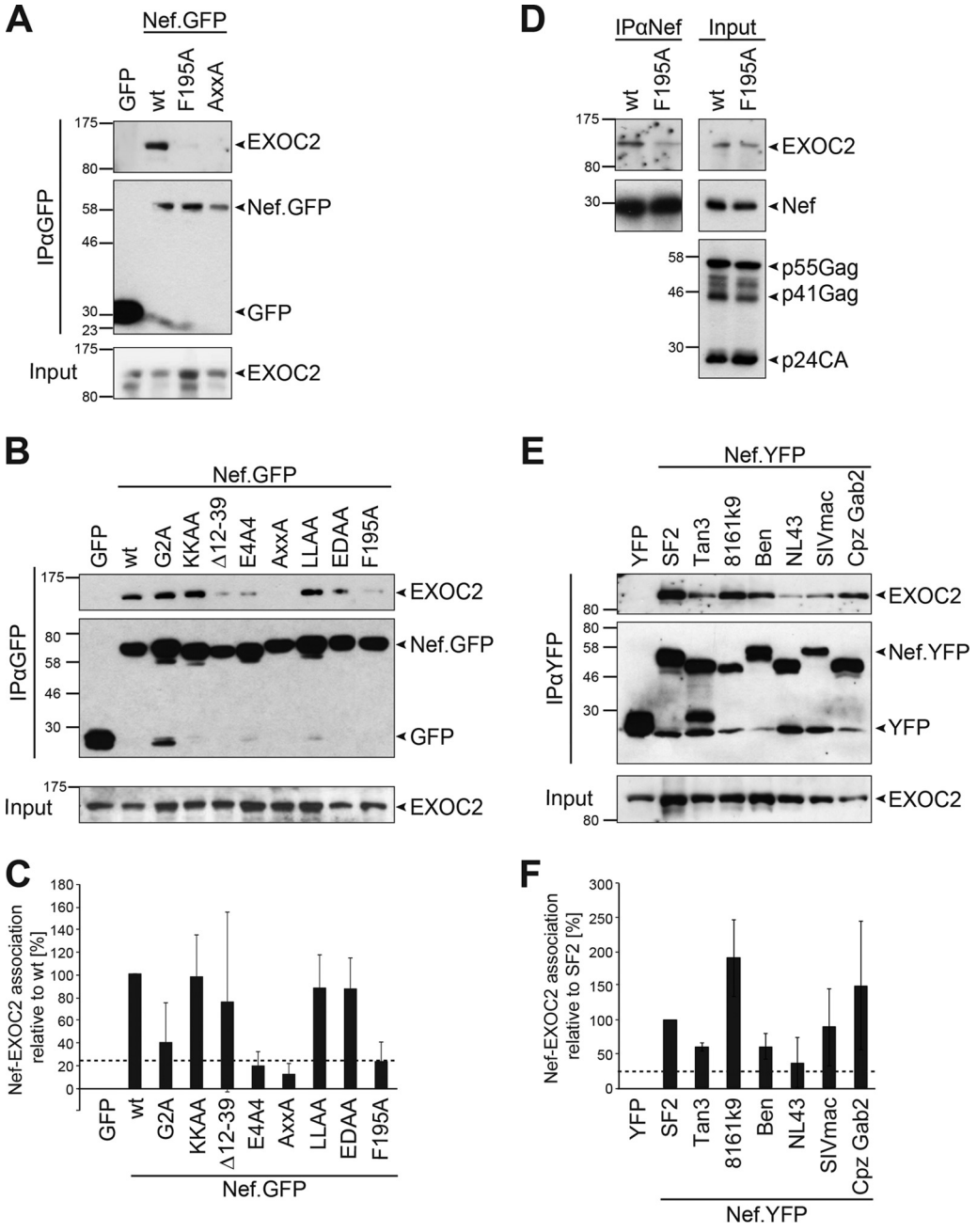

FIG 1 Interactions of Nef with EXOC via the PAK2 association site occur in HIV-infected cells and are conserved among lentiviral Nef proteins. (A and B) Mapping of HIV-1 Nef determinants for EXOC association. Jurkat T lymphocytes (Jurkat TAg) were transfected with constructs encoding GFP, SF2 Nef.GFP, or Nef.GFP mutant proteins, and at 24 h posttransfection, cells were lysed and subjected to immunoprecipitation with GFP-Trap beads. Input and immunoprecipitate (IP) samples were analyzed by SDS-PAGE and Western blotting. Note that, e.g., G2A mutant Nef in panel B is enriched in the immunoprecipitates relative to the WT and thus displays reduced EXOC binding. (C) Quantification of relative coimmunoisolated EXOC2 as shown in panel B. Percentages of coimmunoprecipitated EXOC2 and immunoprecipitated GFP were calculated relative to the percentage of SF2 WT Nef, which was set to 100%. Depicted are means ± standard deviations of up to seven independent experiments. (D) Coimmunoprecipitation of Nef and EXOC from HIV-1-infected cells. Jurkat T (CCR7) cells were infected with WT HIV-1 or the isogenic HIV-1 strain expressing F195A mutant Nef and subjected to immunoprecipitation with a sheep anti-Nef antibody. (E and F) Nef-EXOC association for different HIV-1, HIV-2, and SIV Nef alleles. Coimmunoprecipitation analysis (analogous to that in panel A) of Jurkat TAg cells transiently expressing the indicated YFP or Nef.YFP protein with corresponding quantification (F) of three independent experiments with means ± standard deviations indicated. Nef and EXOC2 association is considered when at least 25% of SF2 WT Nef, which is indicated by dashed lines. The values to the left of the blots are molecular sizes in kilodaltons.

required for Nef-PAK2 association (22, 67). Overall, the molecular determinants for association with EXOC and PAK2 seem to overlap in both the 5C and SF2 Nef proteins. Disruption of the myristoyl acceptor G2, which reduces the association of Nef with cellular membranes (68), weakened Nef's association with EXOC (G2A mutant Nef, 39.8% ± 34.9% [68], 82% in Fig. 1B; see Fig. S2 in the supplemental material for examples of experiments with more strongly reduced coimmunoprecipitation of G2A mutant

Nef with EXOC2). Residues that mediate the incorporation of Nef into membrane microdomains (KKAA [68]) or association with components of the endocytic machinery (LLAA, EDAA [69, 70]) were dispensable for this interaction. Disruption of the interaction motif with the Nef-associated kinase complex (Δ12-39) (71) resulted in variable EXOC interaction efficiency (also see Fig. S2 in the supplemental material).

Importantly, F195-dependent association of SF2 Nef with EXOC2 was also observed when the viral protein was isolated with a Nef-specific antibody from Jurkat T lymphocytes infected with HIV-1 (Fig. 1D). The ability to associate with EXOC2 was a conserved property of lentiviral Nef-yellow fluorescent protein (YFP) from HIV-1 (SF2, NL4.3, 8161k9), HIV-2 (Ben), and SIV (mac239, Cpz Gab2, Tan3), which were previously validated to exert biological Nef activities (17, 25, 35). This conserved binding demonstrated that while F195 is critical for this association of SF2 Nef, other Nef alleles contain binding interfaces that do not contain such a critical phenylalanine residue (see Fig. S1A in the supplemental material). The efficiency of the interaction varied between different Nef alleles but was above the residual binding observed with SF2 Nef PAK2 binding-deficient mutant proteins (relative Nef-EXOC2 associations ranging from 36.0% ± 36.4% for NL4.3 to 190.0% ± 56.4% for 8161k9). Among the limited number of alleles tested, the efficiency of the interaction with EXOC correlated with (i) that of the association with PAK2 activity (see Fig. S1B and C) (35) and, similar to PAK2 association (72), (ii) with an R-to-T polymorphism at the position upstream of the second proline of Nef's proline-rich motif (see Fig. S1A). We conclude that Nef-EXOC interactions in T lymphocytes require the interaction surfaces mediating Nef association with PAK2 but not others of its known protein interaction motifs, occur in the context of HIV-1 infection, and are conserved in lentiviral evolution.

PAK2 is essential for the association of Nef with EXOC. Because of the striking overlap between the determinants involved in Nef's association with PAK2 and EXOC and the correlation of binding efficiency among Nef alleles, we investigated whether the presence of PAK2 has an impact on the ability of Nef to associate with EXOC. To this end, we generated stable Jurkat cells expressing an unrelated control short hairpin RNA (shRNA; Jurkat shCon) or an shRNA targeting PAK2 expression (Jurkat shPAK2) (Fig. 2A). In Jurkat shCon cells, all of the EXOC subunits reported to interact with Nef (EXOC1 to EXOC4) (53) were detected in Nef.GFP immunoprecipitates. In sharp contrast, Nef-EXOC association was almost completely abrogated in Jurkat shPAK2 cells in which PAK2 expression was undetectable by Western blotting. These results indicate that PAK2 is essential for the association of Nef with EXOC.

To gain insight into the molecular mechanism by which PAK2 facilitates the association of Nef with EXOC, we examined the molecular determinants of PAK2 required for this effect. To this end, we generated shPAK2-resistant expression constructs for well-established mutant PAK2 proteins with defects in individual functionally relevant amino acid motifs (48) (Fig. 2B) and tested these proteins for the ability to reconstitute Nef-EXOC association in Jurkat shPAK2 cells. As before (Fig. 2A), only residual association of Nef.GFP with EXOC2 was observed in Jurkat shPAK2 cells (Fig. 2C). Robust Nef-EXOC2 interaction was rescued upon the introduction of shRNA-resistant WT PAK2, as well as most of the mutant PAK2 proteins analyzed. Somewhat surprisingly, reconstitution of Nef-EXOC association was also achieved with catalytically inactive K278R mutant PAK2. Consistent with the dispensability of PAK2 kinase activity for the assembly of Nef-EXOC complexes, the PAK2 kinase inhibitor IPA3 reduced Nef-associated PAK2 activity but did not affect Nef-EXOC association (see Fig. S3 in the supplemental material). In contrast, the H82L/H85L and ISP (I74N/S75P/P77A) mutant PAK2 proteins completely failed or were significantly impaired in reconstituting Nef-EXOC interaction, respectively. These mutations disrupt the interaction of PAK2 with the GTPases Rac1/Cdc42 and thereby keep PAK2 in an autoinhibited, dimerized conformation (73). To distinguish between the impact of GTPase-binding and autoinhibited conformations of PAK2 for facilitating the interaction of Nef with EXOC, the H82L/H85L and L106F mutations were combined to result in a GTPase binding-deficient but conformationally active PAK2 variant (73) (Fig. 2D). Since this mutant protein failed to establish efficient association of Nef with EXOC, we conclude that Nef-associated PAK2 facilitates the assembly of Nef-EXOC complexes via its ability to interact with small GTPases but not via its kinase activity or conformational switching.

EXOC does not affect downstream functions of Nef-associated PAK2. To test the influence of EXOC on Nef-PAK2 association, we attempted to generate shRNA lines lacking the expression of individual EXOC subunits but failed to generate viable cells with stably reduced EXOC expression levels (data not shown). Transient small interfering RNA (siRNA)-mediated silencing of EXOC4 and EXOC2 significantly reduced the expression but did not completely deplete these EXOC subunits, and knockdown of one EXOC subunit frequently decreased the expression levels of other subunits (Fig. 3A, input; see Fig. S7A in the supplemental material). This reduction of EXOC expression levels markedly decreased the association of Nef with EXOC. Under these conditions, Nef's association with PAK2 activity, as scored by autophosphorylation of PAK2 following immunoprecipitation of Nef in an IVKA, was also reduced but still clearly detectable. The Nef-PAK2 IVKA measures the stability of Nef-PAK2 complexes; however, also shorter-lived Nef-PAK2 complexes can be fully functional when assessing the phosphorylation of the PAK2 substrate cofilin (35). To more precisely determine whether EXOC is relevant for downstream functions of the Nef-PAK2 complex, we therefore assessed the ability of Nef to induce high levels of inactive p-cofilin in Jurkat T lymphocytes upon the silencing of PAK2, EXOC2, or EXOC4 (Fig. 3B and C). Expectedly (31), p-cofilin levels of GFP-expressing control cells were only rarely elevated relative to those of untransfected neighboring cells (23.4% ± 5.2% of cells with high p-cofilin levels, see also Fig. S4A in the supplemental material for dual-color images), while cells expressing SF2 Nef.GFP frequently displayed high p-cofilin levels (80.8% ± 5.2% of cells). Silencing of PAK2 expression largely eliminated this Nef effect (40.6% ± 0.7% of cells with high p-cofilin). In contrast, treatment with siEXOC2 or siEXOC4 had no effect on the induction of p-cofilin by Nef.GFP (82.1% ± 6.6% and 83.0% ± 0.9% of cells, respectively). Similar results were obtained when analyzing the inhibitory effect of Nef on chemokine-mediated remodeling of the plasma membrane and chemotaxis (Fig. 3D to F). Stimulation of T cells with the chemoattractant stromal cell-derived factor 1α (SDF-1α) induces the formation of pronounced F-actin-rich cell protrusions (actin ruffles). Actin ruffling is necessary for directional migration toward a chemokine gradient, and the formation of these protrusions is inhibited by Nef (29, 31) (Fig. 3D). Whereas the majority of control GFP-positive cells dis-

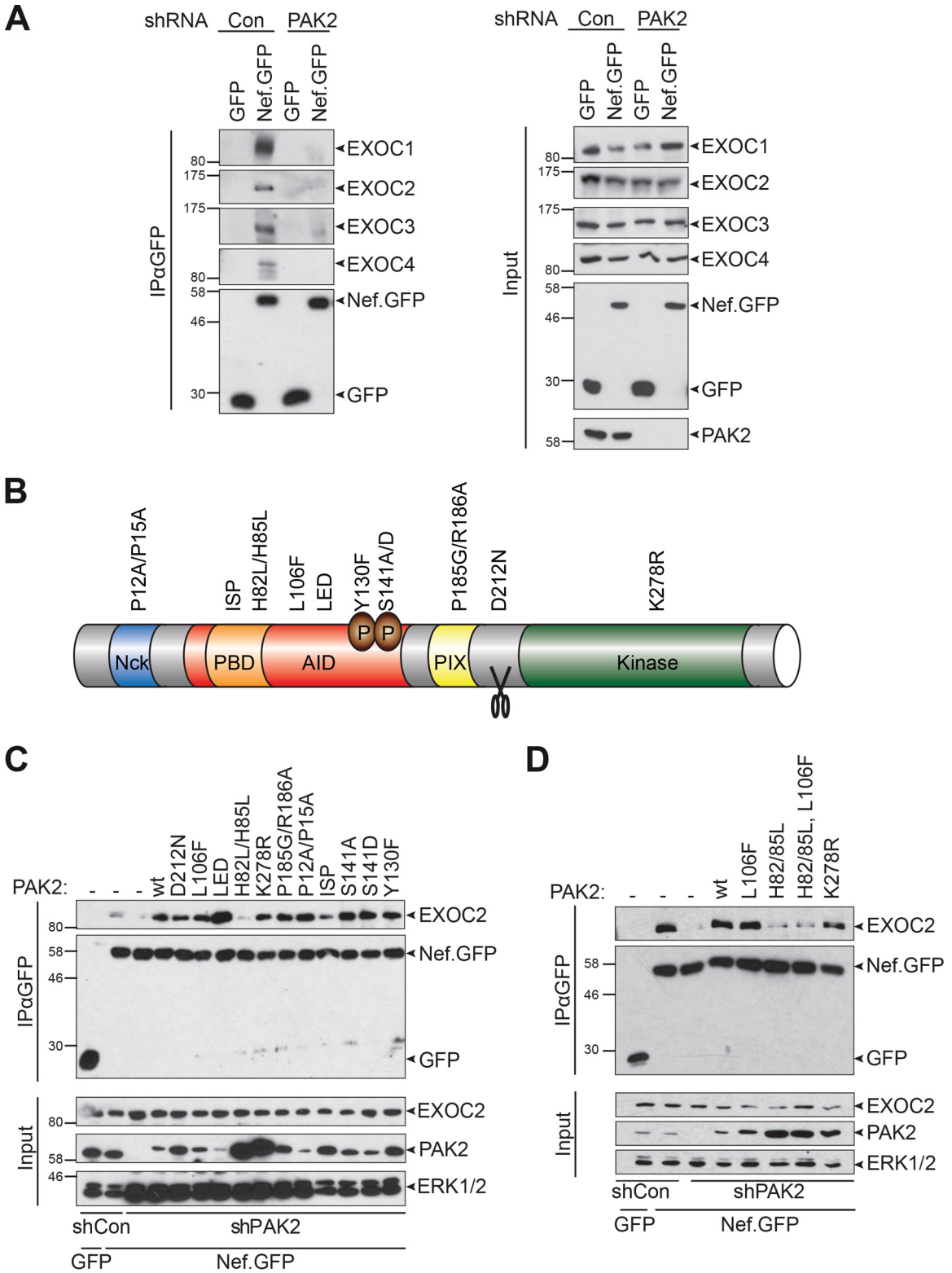

FIG 2 The GTPase interaction site of PAK2 is essential to facilitate interactions of Nef with EXOC. (A) Nef-EXOC coimmunoprecipitation as in Fig. 1 from Jurkat shCon and Jurkat shPAK cells transiently expressing GFP or SF2 Nef.GFP. (B) Schematic illustration of the domain organization and functionally relevant residues of PAK2. The ISP (I74N/S75P/P77A) and H82L/H85L mutant PAK2 proteins lack binding to Rac/Cdc42 because of disruption of the p21 binding domain (PBD). The L106F and K278R mutations partially disrupt PAK2 autoinhibition or abolish PAK2 activity, respectively. AID, autoinhibitory domain. (C and D) Reconstitution of Nef-EXOC coimmunoprecipitation in Jurkat shPAK2 cells by expression of shRNA-resistant PAK2 variants. Coimmunoprecipitation as in panel A but upon transient coexpression of the indicated PAK2 variants. The values to the left of the blots are molecular sizes in kilodaltons.

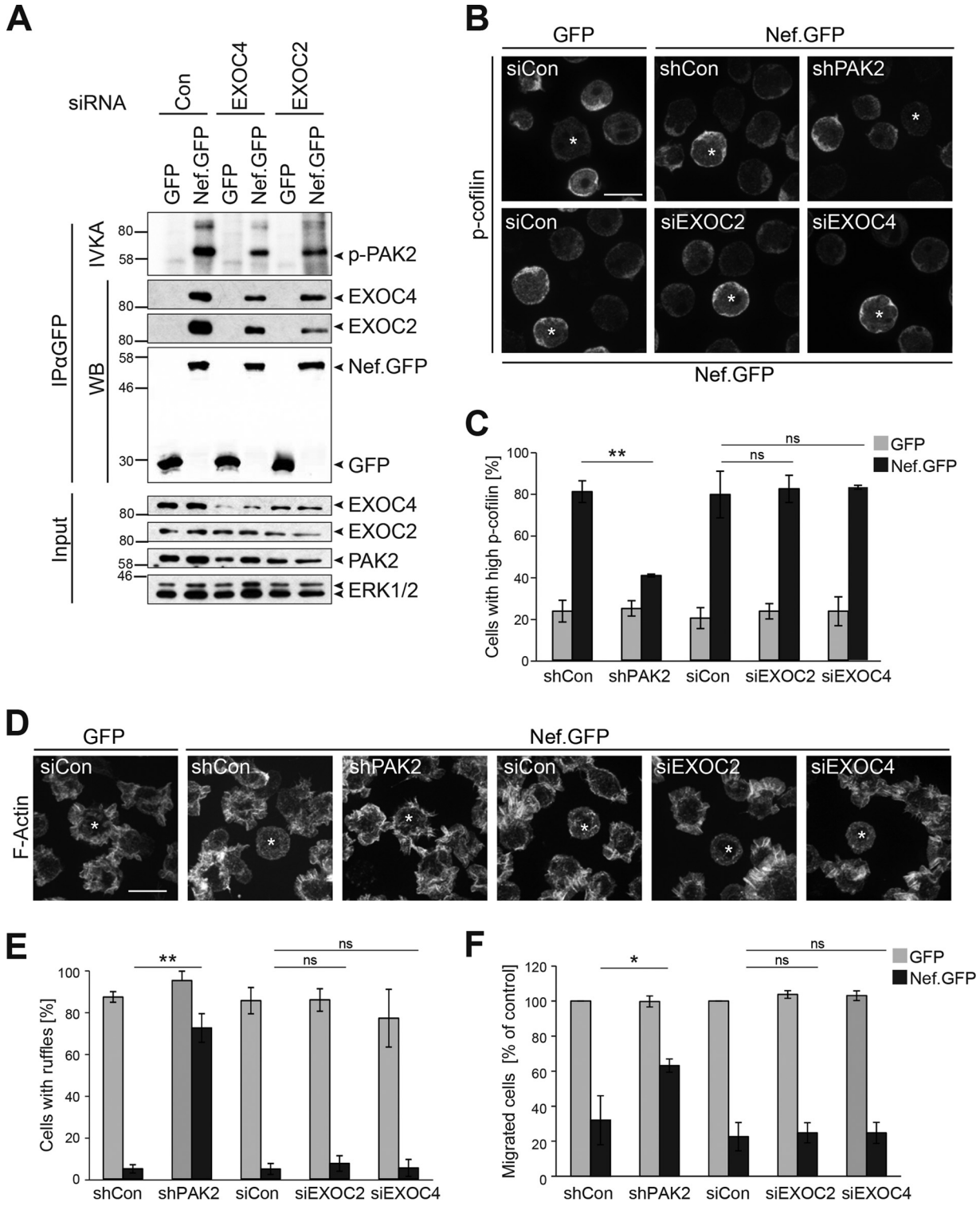

FIG 3 EXOC does not affect Nef-PAK2 downstream functions. (A) Nef-associated PAK2 activity. Jurkat T (TAg) lymphocytes were transfected with siRNA pools targeting EXOC2 or EXOC4 or the respective siRNA control and retransfected with a GFP or SF2 Nef.GFP expression plasmid 48 h later. At 24 h after DNA transfection, cells were lysed and subjected to GFP-Trap immunoprecipitation with subsequent IVKA. Samples were analyzed by SDS-PAGE and subjected to autoradiography and Western blotting to reveal the association of Nef with PAK2 activity (resulting in autophosphorylation of the kinase) and EXOC, respectively. The values to the left of the blots are molecular sizes in kilodaltons. (B and C) Induction of inactive p-cofilin by Nef. (B) Representative confocal micrographs of Jurkat T (CCR7) lymphocytes transiently expressing GFP or Nef.GFP in the context of shRNA-mediated depletion of PAK2, siRNA-mediated reduction of EXOC2 or EXOC4, or the respective control. Cells were plated onto coverslips, fixed, permeabilized, and stained for p-cofilin. Asterisks indicate GFP-positive cells. Scale bar, 10 μm. For dual-color images, see Fig. S4A in the supplemental material. (C) Frequency of the cells shown in panel B with high p-cofilin levels. Depicted are mean values ± standard deviations of three independent experiments with at least 100 cells counted per condition. (D and E)

(Continued)

played such chemokine-induced ruffles (86.9% ± 2.5% of cells; see also Fig. S4B in the supplemental material for dual-color images), expression of Nef.GFP potently reduced the fraction of ruffling cells (4.9% ± 2.0% of cells). While silencing of PAK2 expression almost fully restored the formation of actin ruffles in Nef.GFP-expressing Jurkat cells (72.2% ± 6.6%), silencing of EXOC2 or EXOC4 had no effect (7.4% ± 3.7% and 5.3% ± 4.1%, respectively) (Fig. 3E). Consistently, silencing of PAK2, but not of EXOC, partially restored the chemotaxis of Nef.GFP-expressing Jurkat T cells toward SDF-1α in a transwell migration assay (63.2% ± 3.8% of shPAK2-treated cells versus 24.8% ± 5.7% of siEXOC2-treated cells or 24.8% ± 6.0% siEXOC4-treated cells, Fig. 3F). Together, these results suggest that EXOC stabilizes the association of Nef with PAK2 but is not essential for the induction of downstream functions of Nef-PAK2 complexes.

EXOC is dispensable for deregulation of trafficking of host transmembrane and peripheral membrane proteins by Nef. To investigate which biological activities of Nef involve EXOC, we first addressed the downregulation of cell surface receptors. To this end, we transiently expressed GFP or SF2 Nef.GFP in Jurkat T cells and determined relative cell surface protein levels as the mean receptor intensity of highly expressing cells as a percentage of that of untransfected cells in the same sample. Values are expressed relative to those in GFP-positive control cells, which were set to 100% (Fig. 4) (9). This allowed us to determine the effect of ectopic viral gene expression on the relative steady-state surface exposure of each receptor analyzed. In the case of CD4, Nef.GFP induced a potent reduction of cell surface exposure to approximately 30% of that of GFP-expressing control cells, despite the heterogeneous levels of this receptor on the surfaces of the cells used (Fig. 4A). Similar CD4 downregulation by Nef.GFP was observed upon the reduction of PAK2, EXOC2, or EXOC4 expression (Fig. 4B). Downregulation of cell surface CXCR4 (Fig. 4C and D) and major histocompatibility complex class I (MHC-I) (Fig. 4E and F), which is less pronounced than downregulation of CD4 and occurs via distinct molecular mechanisms (7, 74), was also largely unaffected upon the silencing of PAK2 or EXOC expression. Only for MHC-I downregulation did we observe a mild effect of PAK2 silencing (60.4% ± 6.6% of MHC-I expression compared to 38.2% ± 5.7% in matched controls), while silencing of EXOC had no effect. Finally, we assessed retargeting of the peripheral membrane protein Lck from the plasma membrane to an intracellular compartment previously identified as the TGN, which results from a Nef-mediated block of anterograde transport of newly synthesized and recycling Lck protein (16, 24, 75). As expected, Lck prominently localized to the plasma membrane with virtually no accumulation in intracellular compartments in GFP-expressing control Jurkat T lymphocytes (1.3% ± 0.6% cells with Lck accumulation in the TGN) (Fig. 4G; see Fig. S4C in the supplemental material for dual-color images) and Nef.GFP triggered potent intracellular accumulation of the kinase in a large majority of the cells (97.1% ± 3.0% of cells with Lck accumulation in the TGN). This Nef-mediated retargeting of Lck was fully preserved in cells with reduced expression of PAK2, EXOC2, or EXOC4. We conclude that interactions of Nef with PAK2 and EXOC are not involved in the Nef-mediated misrouting of host cell receptors and peripheral membrane proteins.

EXOC is involved in the inhibition of TCR-induced actin remodeling by Nef. T cell activation is governed primarily by signaling elicited by engagement of the TCR in a tight contact with antigen-presenting cells referred to as the immunological synapse (IS) (76). TCR engagement by specific MHC-presented peptides launches highly dynamic and coordinated transport events that recruit specific factors to the IS and exclude others from it. This signal initiation triggers a broad cascade of downstream signaling that includes dynamic F-actin remodeling at the IS, tyrosine phosphorylation, and release of calcium flux, which are coordinated to trigger transcriptional profiles, including induced expression of the T-cell survival cytokine interleukin-2 (77). Many aspects of these events can be simulated when applying T lymphocytes to a surface that triggers TCR signaling, e.g., by coating with anti-CD3 antibodies. T lymphocytes adhere to and rapidly spread on the substratum under these conditions, and these processes are paralleled by marked remodeling of F-actin into pronounced circumferential F-actin rings. While HIV-1 Nef does not affect T lymphocyte adhesion on such stimulatory surfaces, cell spreading and formation of circumferential F-actin rings are strongly inhibited by the viral protein in an F195-dependent manner (22, 23, 26). As expected, expression of Nef.GFP in Jurkat T lymphocytes treated with control siRNA or shRNA resulted in small cells with little peripheral F-actin, thus reducing the frequency of cells that formed circumferential F-actin-rich rings (25.5% ± 4.2% and 34.3% ± 8.1% of cells, respectively) (Fig. 5A and B; see Fig. S5 in the supplemental material for more examples and dual-color images). This Nef-mediated block of TCR-induced cell spreading and actin polymerization was almost completely abolished in Jurkat shPAK2 cells (78.5% ± 2.0% in Nef-expressing shPAK2 cells versus approximately 92.8% ± 4.0% in GFP shCon). Importantly, silencing of EXOC2 or EXOC4 also significantly increased the frequency of Nef.GFP-expressing cells with circumferential F-actin-rich rings (56.9% ± 11.6% and 67.1% ± 11.3%, respectively). Four morphotypes could be distinguished under these experimental conditions (Fig. 5C, inset): fully spread cells with a circumferential F-actin ring (black bars, prototypic of GFP-expressing cells), incompletely spread cells with a circumferential F-actin ring (dark gray bars), fully spread cells lacking circumferential F-actin polymerization (light gray bars), and cells that failed to spread and lacked a circumferential F-actin ring (white bars,

Figure Legend Continued

Inhibition of chemokine-induced actin ruffling by Nef. (D) Representative maximum projections of confocal Z-stacks of GFP- or Nef.GFP-expressing Jurkat T (CCR7) lymphocytes upon silencing of PAK2 or EXOC expression. Cells were used to seed coverslips at 24 h posttransfection with expression constructs, stimulated with 200 ng/ml SDF-1α for 20 min, fixed, permeabilized, and stained with phalloidin-TRITC to visualize F-actin. Asterisks indicate GFP-positive cells. Scale bar, 10 μm. For dual-color images, see Fig. S4B in the supplemental material. (E) Frequency of cells shown in panel D with chemokine-induced ruffles. Depicted are mean values ± standard deviations of three independent experiments with at least 100 cells counted per condition. (F) Chemotaxis toward SDF-1α. Cells shown in panel D were starved and allowed to migrate through a 5-μm porous transwell filter toward an SDF-1α gradient for 2 h. Migrated cells were quantified by flow cytometry, and data are plotted relative to the corresponding GFP control, which was set to 100%. Depicted are mean values ± standard deviations of three independent experiments each performed in triplicate. Statistical significance was assessed by Student's *t* test. ns, not significant; *, $P < 0.05$; **, $P < 0.01$.

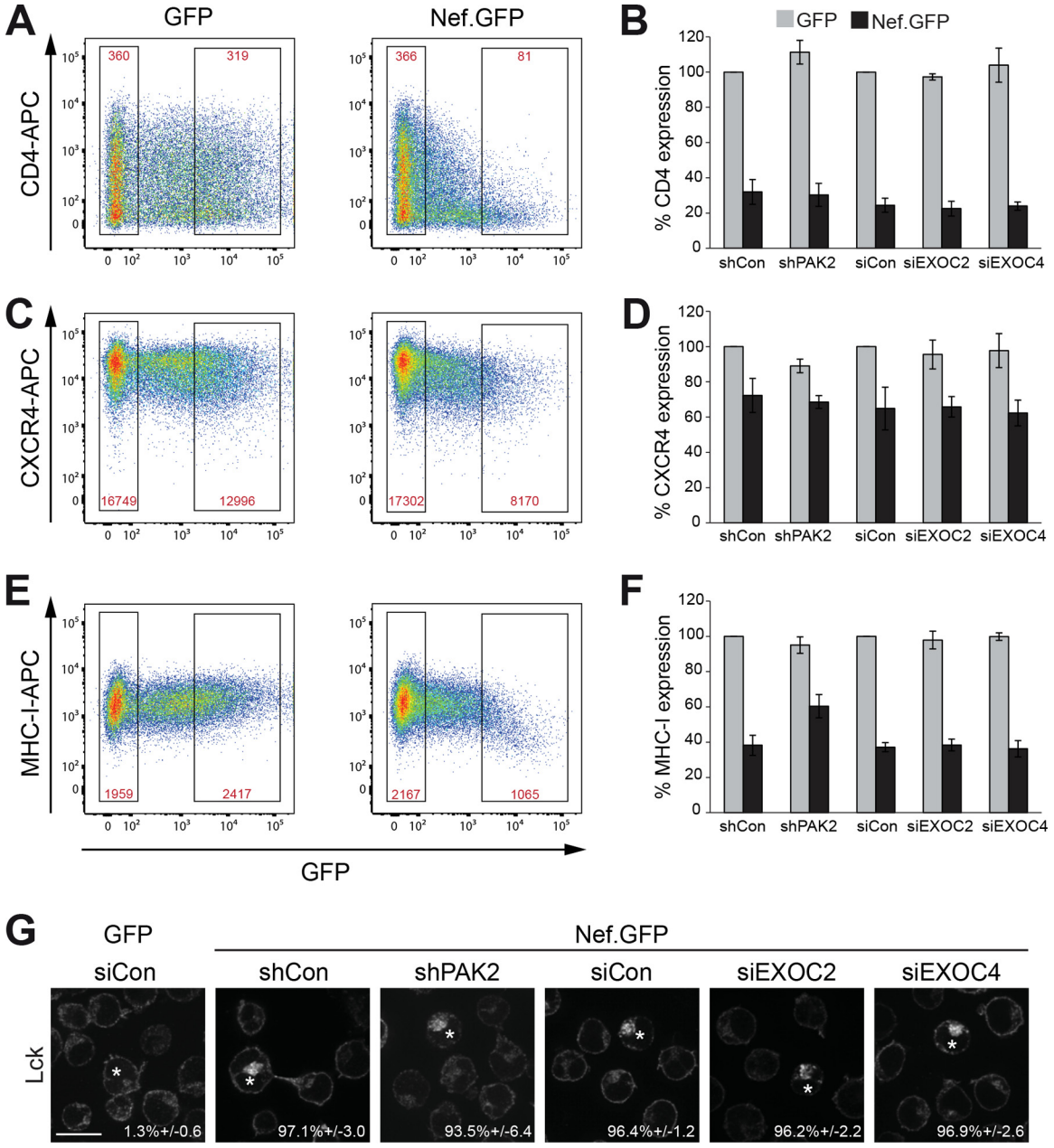

FIG 4 EXOC does not affect Nef-mediated perturbations of host cell vesicular transport. (A) Cell surface CD4 levels. Jurkat T (CCR7) lymphocytes transiently expressing GFP or SF2 Nef.GFP were stained with allophycocyanin (APC)-conjugated antibodies against CD4 and analyzed by flow cytometry. Gates of live nontransfected and highly expressing cells are indicated. Red values are the mean fluorescence intensities of the CD4 signals in the respective gates. (B) Quantification of relative CD4 cell surface levels as shown in panel A. Mean fluorescence intensity percentages of highly expressing and nontransfected cells treated with shRNA or siRNA, as indicated, were calculated relative to the corresponding GFP control, which was set to 100%. Displayed are the mean values ± the standard deviations from three independent experiments. (C and D) Cell surface CXCR4 levels. Primary fluorescence-activated cell sorting (FACS) plots (C) and quantification (D) of cell surface CXCR4 levels as detected by APC-conjugated antibodies to CXCR4. (E and F) Cell surface MHC-I levels. Primary FACS plots (E) and quantification (F) of cell surface MHC-I levels as detected by APC-conjugated antibodies to MHC-I. (G) Representative confocal micrographs of Jurkat T (TAg) lymphocytes expressing GFP or Nef.GFP in the context of shRNA-mediated depletion of PAK2, siRNA-mediated reduction of EXOC2 or EXOC4, or the respective control. Cells were plated onto coverslips, fixed, permeabilized, and stained for endogenous Lck, which accumulates in the TGN in the presence of Nef. Asterisks designate GFP-positive cells. Values are the mean percentages ± the standard deviations of cells with intracellular Lck accumulation from three independent experiments. Scale bar, 10 μm. For dual-color images, see Fig. S4C in the supplemental material.

prototypic of Nef.GFP-expressing cells). Silencing of PAK2 mostly resulted in Nef.GFP-expressing cells that spread well with prominent F-actin rings (black bars, 66.3% of cells) and were undistinguishable from GFP-expressing control cells. In contrast, reduced expression of EXOC components often resulted in Nef.GFP cells that failed to fully spread on the stimulatory surface but displayed pronounced circumferential actin rings (32.4% and 29.8% of cells for siEXOC2 and siEXO4, respectively) (Fig. 5A and

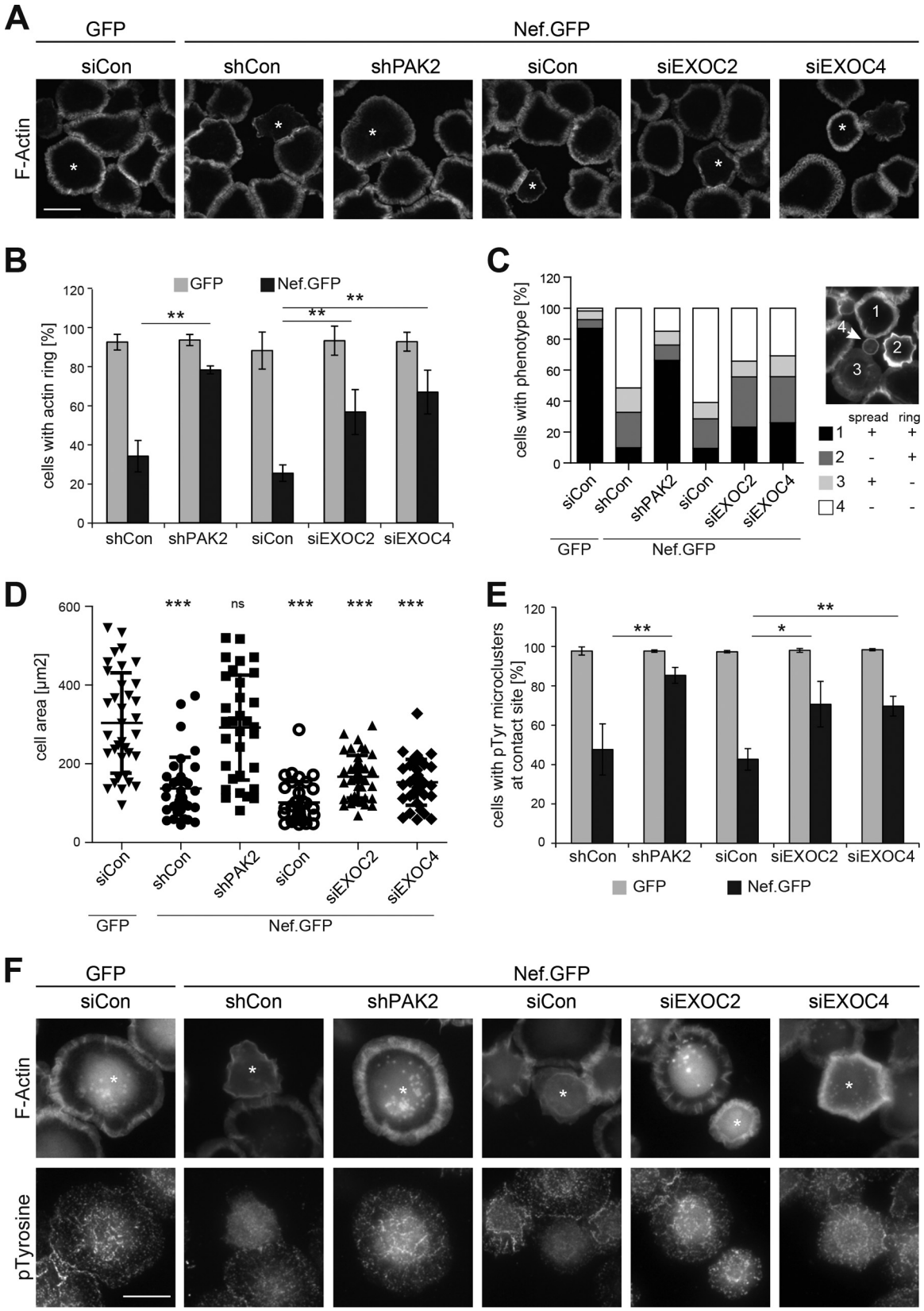

FIG 5 EXOC facilitates inhibition of T cell receptor-induced actin rearrangements by Nef. (A) Representative confocal micrographs of Jurkat T lymphocytes (Jurkat TAg) plated onto stimulatory coverslips for the induction of F-actin rings. Cells were treated with shRNA or siRNA, as indicated, prior to transfection with GFP or SF2 Nef.GFP expression plasmids. Four minutes after being plated onto anti-CD3ε-coated coverslips, cells were fixed and permeabilized and F-actin was

(Continued)

C). Quantification of the total cell spreading area confirmed that PAK2 was critical for the inhibition of T cell spreading by Nef, while EXOC had only moderate effects on this parameter (Fig. 5D). Live cell imaging for extended times revealed that these observed defects in cell spreading persisted over time (see Fig. S6 in the supplemental material), indicating that Nef not only delays but blocks the spreading process in an EXOC-independent manner. Cell spreading and actin remodeling upon TCR engagement are prerequisites for proximal TCR signaling, which is characterized by a burst in tyrosine phosphorylation, a process that is efficiently inhibited by Nef (19, 23, 26). Consistent with the findings on F-actin ring formation, PAK2 and EXOC were required for this block in tyrosine phosphorylation by Nef (Fig. 5E and F). These results imply that interactions with EXOC facilitate the inhibition of TCR-induced actin remodeling and proximal signaling by Nef. In order to dissect further the contribution of PAK2 and EXOC to the Nef-mediated inhibition of TCR-triggered actin remodeling, several shRNA-resistant mutant PAK2 proteins analyzed earlier for the ability to reconstitute Nef-EXOC interaction in Jurkat shPAK2 cells were analyzed for TCR-induced T cell spreading/actin remodeling (see Fig. S7B and C in the supplemental material). As expected, WT PAK2 reconstituted efficient inhibition of T cell spreading and formation of circumferential F-actin rings by Nef (19.8% ± 14.9% of cells). In contrast, kinase-dead K278R mutant PAK2 failed to support this Nef activity (72.7% ± 11.9% of cells), demonstrating that kinase activity, presumably via the inactivation of cofilin, is essential for this process. Since K278R mutant PAK2 still enables Nef to associate with EXOC, this result also implies that Nef-EXOC interactions are not sufficient to explain the observed inhibition of TCR-induced actin ring formation by Nef. Consistently, H82L/H85L mutant PAK2, which, because of a lack of GTPase interaction, fails to trigger Nef-EXOC association and does not enable kinase activation, also did not support inhibition of TCR-induced actin remodeling by the viral protein (65.0% ± 12.6% of cells). These results establish interaction with EXOC as a novel and necessary step in the inhibition of Nef-mediated inhibition of TCR-induced actin remodeling that depends on prior Nef-PAK2 association and synergizes with the effects exerted by the kinase activity of PAK2.

DISCUSSION

Inhibition of host cell actin remodeling constitutes one of the conserved activities of lentiviral Nef proteins by which activation status and motile behavior of infected cells in response to extracellular stimuli are modulated to optimize virus replication in the infected host. These activities were thought to rely exclusively on the conserved association of Nef with the host cell kinase PAK2, which, upon association with the viral protein, inactivates the actin-severing factor cofilin by phosphorylation. Association of HIV-1 SF2 Nef with PAK2 depends on an interaction site involving the critical residue F195, for which, until recently, PAK2 was the only cellular ligand identified. The description of EXOC as an additional interaction partner that depends on residues required for PAK2 association raised questions regarding the specificity of this interaction site, the potential mutual impact of PAK2 and EXOC on each other, and the relevance of EXOC for Nef function. In our attempts to address these issues, we have confirmed that HIV-1 Nef interacts with EXOC via its PAK2 interaction site, detected this interaction in the context of HIV-1 infection, and established the Nef-EXOC association as a feature that is conserved in lentiviral evolution. Surprisingly, the presence of PAK2 was strictly required for detection of the Nef-EXOC association. This did not require PAK2 kinase activity but depended on residues mediating its interaction with Rac1/Cdc42 GTPases. In turn, EXOC had only a moderate effect on the ability of Nef to associate with PAK2 activity, was dispensable for direct downstream effects of Nef-PAK2 complexes on cofilin and chemokine-induced actin dynamics, and did not mediate effects of Nef on host cell vesicular transport. Functional relevance of EXOC was observed for the Nef-mediated disruption of T cell responses to TCR engagement, where EXOC was critical for the disruption of actin remodeling and proximal TCR signaling.

Our results are most compatible with a model in which Nef associates with PAK2 and EXOC in a sequential manner, where the initial association with PAK2 facilitates Nef's subsequent interaction with EXOC (see Fig. S8 in the supplemental material). In this scenario, transient Nef-PAK2 complexes are assembled in which PAK2 is in its active phosphorylated state because of the presence of the GTPases Rac1/Cdc42 and their guanine exchange factor Vav in the complex. Once PAK2 is dissociated from the complex, its substrate specificity is altered, leading to phosphorylation of cofilin and possibly additional substrates such as paxillin (78) to impair host cell actin-remodeling events, including TCR-induced cell spreading and actin polymerization. The GTPase Cdc42, which interacts with PAK2 within Nef-PAK2 complexes, also associates with EXOC (55, 56) and can recruit it for the formation of Nef-EXOC complexes. On the basis of the abundance of Nef-EXOC complexes that, in contrast to Nef-PAK2 complexes, can easily be coimmunoprecipitated and detected by Western blotting, associations of Nef with EXOC appear to be relatively

Figure Legend Continued

stained with phalloidin-TRITC. Asterisks indicate GFP-positive cells. Scale bar, 10 μm. Further examples and dual-color images are provided in Fig. S5. (B) Frequency of cells with circumferential F-actin rings shown in panel A. Displayed are mean values ± standard deviations of three independent experiments with at least 100 cells counted per condition. (C) Stratification of cells shown in panel A into four different morphotypes based on F-actin ring formation and cell spreading. The different morphotypes are depicted in the inset as follows: 1, fully spread cells with a circumferential F-actin ring (black bars); 2, incompletely spread cells with a circumferential F-actin ring (dark gray bars); 3, fully spread cells lacking circumferential F-actin polymerization (light gray bars); 4, cells that failed to spread and lacked a circumferential F-actin ring (white bars). The graph is representative of three independent experiments with at least 100 cells counted per condition. (D) Single-cell analysis of the cell areas of the cells shown in panel A. Single-cell areas were manually determined from micrographs by ImageJ. Thirty to 40 cells with high GFP expression were randomly chosen and analyzed. Data points represent single-cell areas. Mean values ± standard deviations are indicated, and the Mann-Whitney U test was used to determine significant differences from siCon GFP. (E and F) EXOC facilitates inhibition of proximal TCR signaling by Nef. (E) Frequency of cells with pTyr microclusters shown in panel F. Displayed are mean values ± standard deviations of three independent experiments with at least 100 cells counted per condition. (F) Representative wide-field micrographs of Jurkat T (TAg) lymphocytes plated onto stimulatory coverslips for the induction of F-actin rings and p-tyrosine microclusters. Cells were treated as described for panel A. Cells were stained with phalloidin-Alexa Fluor 350 and rabbit anti-p-tyrosine antibodies and detected with Alexa Fluor 568-conjugated anti-rabbit antibody. Asterisks indicate GFP-positive cells. Scale bar, 10 μm. ns, not significant; *, $P < 0.05$; **, $P < 0.01$; ***, $P < 0.001$.

stable. This also suggests that PAK2 facilitates the formation of Nef-EXOC complexes by virtue of its transient association with Nef rather than acting as an integral component of Nef-EXOC complexes. We thus propose that PAK2 acts as an adaptor protein to facilitate the formation of Nef-EXOC complexes and, once dissociated from Nef, as a direct Nef effector via its kinase activity. In this scenario, PAK2 activity and EXOC are both necessary but not sufficient for the inhibition of TCR-induced actin remodeling and proximal signaling by Nef. This is in contrast to the inhibition of T lymphocyte actin remodeling and motility in response to chemokines, which, as shown here, requires only the association of Nef with PAK2 activity and not the subsequent formation of complexes with EXOC. Why EXOC is specifically involved in actin remodeling triggered by TCR but not chemokine receptor engagement remains an important topic of future studies. At this point, we speculate that the involvement of EXOC may be warranted for the inhibition of processes that polarize toward the trigger (TCR stimulatory surface or IS) while EXOC may be dispensable for nonpolarized processes such as stimulation by a soluble chemokine.

Another central aspect of this study was the characterization of the role of EXOC in biological activities of Nef. Although only moderate and transient reduction of EXOC expression was tolerated in our cell systems, these conditions significantly reduced the efficiency of Nef-EXOC interactions. In contrast to the induction of nanotubes (53), the Nef-regulated processes addressed here were not impaired by reducing EXOC expression in the absence of the viral protein. This indicated that, similar to PAK2, Nef hijacks EXOC to retarget its biological activities, which allowed us to investigate the specific contribution of EXOC to Nef function. This contribution, however, may be somewhat underestimated in these experiments because of the moderate knockdown efficiencies. Silencing of EXOC subunits did not impair the effects of Nef on the subcellular localization of transmembrane (CD4, MHC-I, CXCR4) and peripheral membrane (Lck) proteins. Relocalization of host cell receptors by Nef is often mediated by blocking their anterograde transport and requires the acidic stretch and the proline-rich motif also involved in Nef-EXOC interactions. Considering that a primary function of EXOC consists of tethering exocytic vesicles to the plasma membrane (79), it was somewhat surprising that this complex was not involved in Nef activities targeting anterograde vesicular membrane trafficking. However, this result is consistent with the dispensability of the F195 residue in SF2 Nef for these activities (16, 31, 40). This also implies that Nef's acidic stretch and proline-rich motif function independently to interfere with host cell vesicular transport and actin dynamics. An involvement of EXOC in additional effects of Nef such as triggering of exosome release still remains to be analyzed (80–82).

The identification of EXOC as a novel effector employed by Nef to restrict TCR-induced actin dynamics and signaling is in line with its ability to couple actin dynamics to membrane remodeling (60) and suggests that Nef selectively targets this EXOC function. How Nef achieves this on the molecular level remains to be elucidated. Given that EXOC *per se* was not essential in TCR-induced actin remodeling, the association of Nef with EXOC may regulate the activity of the viral protein rather than affect general EXOC functions. To decipher the underlying mechanism, it will be necessary to identify the direct binding partner of Nef in Nef-EXOC complexes, elucidate the stoichiometry of EXOC when it is in a complex with Nef, and determine the precise subcellular localization of this interaction.

Considering the impact of Nef on HIV replication and disease progression in AIDS patients, it would be important to add antivirals targeting Nef function to current treatment regimens. Although some preliminary progress in this area has been reported (83–85), therapeutic interference with Nef activity is complicated by the lack of enzymatic activity and its mode of action as a multivalent protein interaction adaptor. An alternative strategy might be to interfere with the activities of Nef's interaction partners. Because of their implication in many different types of cancer, PAKs have become a subject of intense drug development efforts (86, 87). The results of our study place PAK2 as the central downstream effector of Nef in the manipulation of host cell actin remodeling, suggesting that PAK2 inhibitors could be suitable for interference with this Nef activity. However, we found that PAK2 facilitated Nef-EXOC interactions independently of its kinase activity. Thus, development of compounds that can block PAK2 adaptor functions may be warranted to interfere with Nef activity, a concept that may also be worthwhile to consider for the inhibition of PAKs in cancer. Irrespective of the mode of PAK2 action, the PAK2 interaction surface in Nef represents an attractive target for therapeutic interference, as it is essential for all downstream effects of Nef-associated PAK2. The major challenge is to identify a single compound that targets this overall conserved yet heterogeneously composed binding pocket across Nef proteins from different HIV-1 subtypes and clades.

Together, our studies have unraveled a novel and surprising role for EXOC in the inhibition of TCR-induced actin remodeling by Nef, an activity implied in the optimization of virus spread and immune evasion *in vivo*. This process is mediated by the stepwise interaction of Nef with PAK2 and EXOC, which synergize in reprogramming the response of T lymphocytes to TCR engagement. The binding pocket in Nef mediating association with PAK2 and subsequently EXOC emerges as an attractive target for future drug development.

MATERIALS AND METHODS

(See Text S1 in the supplemental material for additional Materials and Methods.)

Cell culture and transfection. HEK293T cells were cultivated in Dulbecco's modified Eagle's medium containing 10% fetal calf serum (FCS) and 1% penicillin-streptomycin, which was further supplemented with 1× nonessential amino acids, 1× sodium pyruvate, 10 mM HEPES (pH 7.4), and 45.76 μM β-mercaptoethanol for Jurkat CCR7 cells. Jurkat TAg cells (Jurkat cells expressing the simian virus 40 large T antigen) were maintained in RPMI 1640 supplemented with 10% heat-inactivated FCS and 1% penicillin-streptomycin (RPMI++). For live microscopy, cells were transferred to CO_2-independent imaging medium (RPMI++ without phenol red, 20 mM HEPES, 2 mM sodium pyruvate). Puromycin (4 μg/ml; Sigma-Aldrich) was added for shRNA-transduced T cells to select successfully transduced cells. Jurkat TAg and CCR7 cells were electroporated with 30 to 50 μg of total plasmid DNA per 1×10^7 cells (250 V, 950 and 850 μF, respectively; Bio-Rad Gene Pulser). siRNA transfections were conducted with 500 pmol per 1×10^7 cells, followed at 48 h by the electroporation of GFP or Nef.GFP expression constructs. Cells were subjected to lysis or used for functional assays by immunofluorescence assay or flow cytometry 24 h after DNA transfection.

Immunofluorescence. Responses to TCR engagement were monitored by the formation of circumferential F-actin rings as previously described (23). In brief, stimulatory coverslips were prepared by coating with a 0.01% poly-L-lysine (PLL; Sigma-Aldrich) solution for 10 min at

room temperature, followed by wet-chamber incubation for 3 h at 37°C with 7 μg/ml anti-CD3ε (50 μl per coverslip, clone HIT3a against CD3ε; BD Biosciences) in phosphate-buffered saline (PBS). Stimulatory coverslips were subsequently washed in PBS and stored at 4°C in PBS until use. For all other immunofluorescence analyses, coverslips were coated with PLL for 30 min at 37°C. Transfected Jurkat TAg cells (3×10^5 or 5×10^5 per CD3ε-coated or PLL-coated coverslip, respectively) were used to seed coverslips for 4 min to allow TCR-mediated actin ring formation or for adherence to PLL. For induction of chemokine-induced ruffling, Jurkat CCR7 cells on PLL were additionally allowed to respond to 200 ng/ml SDF-1α (PeproTech) for 20 min. Cells were subsequently fixed in 3% paraformaldehyde for 15 min, permeabilized for 2 min in 0.1% Triton X100, and blocked for 30 min in 1% FCS in PBS. An indirect immunofluorescence assay was performed by incubating the cells with a mouse anti-Lck antibody (clone 3A5; Santa Cruz; 1:50 overnight), a rabbit anti-p-cofilin antibody (clone 77G2; Cell Signaling; 1:50 overnight, all steps in Tris-buffered saline [TBS] instead of PBS), or a rabbit anti-p-tyrosine antibody (clone PY350; Santa Cruz; 1:50 overnight in TBS) and a goat anti-rabbit or goat anti-mouse secondary antibody coupled to Alexa Fluor 568 (1:2,000, 1 h room temperature; Invitrogen). For ruffle induction and actin ring assays, F-actin was visualized with tetramethyl rhodamine isothiocyanate (TRITC)-conjugated phalloidin (1:1,000, 1 h, room temperature; Sigma). Samples were mounted on glass slides with Mowiol and analyzed by epifluorescence (Olympus IX81 S1F-3, cellM software) and confocal (spinning-disc PerkinElmer UltraView VoX, Volocity software) microscopes. Life microscopy of actin ring formation was done with the spinning-disc microscope at 37°C with a 40× objective and 10-μm Z-stacks with a 1-μm interval every 10 s for 10 min. For quantification of phenotype frequencies, at least 100 transfected cells were counted and their phenotype was judged in comparison to that of untreated or untransfected neighboring cells. Single-cell analysis of cell spreading on stimulatory coverslips was performed by manually circling 30 to 40 randomly selected cells with high GFP fluorescence by using ImageJ.

Coimmunoprecipitation. Twenty-four hours posttransfection, cells were counted and adjusted for equal GFP-positive cell numbers. Cells were washed once with PBS and lysed in lysis buffer (1% Triton X-100, 150 mM NaCl, 50 mM Tris HCl [pH 8.0], 1 mM Na_3VO_4, protease inhibitors at 1:1,000 [Sigma]) for 30 min on ice. Lysates were cleared by centrifugation, mixed with 15 μl of equilibrated GFP-Trap beads (Chromotek), and incubated with rotation for 2 h at 4°C. Beads were washed three times with 500 μl of wash buffer (150 mM NaCl, 1% Igepal CA-630 [equivalent to NP-40], 0.5% sodium deoxycholate, 0.1% SDS, 50 mM Tris HCl [pH 8.0]) and once with 100 μl of 20 mM Tris HCl (pH 7.5), and protein was eluted in 30 μl of hot 2× SDS sample buffer and boiled for 5 min. Samples of cleared input and eluates were analyzed by Western blotting. To immunoprecipitate Nef from infected Jurkat CCR7 cells, the above-mentioned protocol was modified as follows. A total of 1×10^7 cells from an infected culture were used per condition, and cell lysates were incubated with sheep anti-Nef antiserum (1:200 ARP444, a gift from M. Harris, Leeds University) for 45 min on ice. Meanwhile, protein A Sepharose beads (GE Healthcare) were blocked with a noninfected cell lysate and washed once in lysis buffer before being combined with the antibody-loaded cell lysates. Quantification of coimmunoprecipitation efficiency was based on the measurement of signal intensity with Quantity One software (Bio-Rad). The percentages of coimmunoprecipitated EXOC and immunoprecipitated GFP signals were calculated and correlated with the percentages obtained for SF2 WT Nef, which were set to 100%.

IVKA. To assess Nef-associated PAK2 activity, standard IVKAs were performed as previously described (35). Nef.GFP was immunoprecipitated from transfected Jurkat TAg cells after lysis in KEB (137 mM NaCl, 50 mM Tris/HCl [pH 8], 2 mM EDTA, 0.5% Nonidet P-40, 1 mM Na_3VO_4, protease inhibitors). Upon incubation with GFP-Trap beads, samples were extensively washed with KEB and resuspended in 50 μl of KAB (50 mM HEPES [pH 8], 150 mM NaCl, 5 mM EDTA, 0.02% Triton X-100, 10 mM $MgCl_2$) containing 10 μCi of [γ-^{32}P]ATP (Hartmann Analytic) per reaction. After 10 min of incubation at room temperature, samples were repeatedly washed in KEB, mixed with 2× SDS sample buffer, and boiled. Bound proteins were separated by SDS-PAGE and subjected to autoradiography. For pharmacological inhibitor experiments, GFP- or Nef.GFP-transfected Jurkat T lymphocytes were incubated for 1 h with 10 μM PAK2 kinase inhibitor IPA3 (catalog no. 3622; Tocris) or its inactive pharmacological control PIR3.5 (catalog no. 4212; Tocris) and then subjected to IVKA.

Statistical analysis. Statistical analysis of data sets was carried out with Microsoft Excel and GraphPad Prism. The statistical significance of parametrically and not normally distributed data sets was analyzed with the Student *t* test and the Mann-Whitney U test, respectively.

SUPPLEMENTAL MATERIAL

Supplemental material for this article may be found at http://mbio.asm.org/lookup/suppl/doi:10.1128/mBio.01309-15/-/DCSupplemental.

Text S1, DOCX file, 0.04 MB.
Figure S1, PDF file, 0.1 MB.
Figure S2, PDF file, 0.1 MB.
Figure S3, PDF file, 0.1 MB.
Figure S4, PDF file, 0.1 MB.
Figure S5, PDF file, 0.5 MB.
Figure S6, PDF file, 0.4 MB.
Figure S7, PDF file, 0.2 MB.
Figure S8, PDF file, 0.1 MB.

ACKNOWLEDGMENTS

This project was supported by the Deutsche Forschungsgemeinschaft (TRR83 projects 8 and 15 to B.H. and O.T.F. and grant FA 378/11-1 to O.T.F.). O.T.F. is a member of the cluster of excellence EXC81.

We are grateful for access to the biosafety level 2 imaging facility of the Nikon Imaging Center, to Vibor Lateka for helpful advice and discussion, and to Mark Harris for the kind gift of reagents.

REFERENCES

1. **Deacon NJ, Tsykin A, Solomon A, Smith K, Ludford-Menting M, Hooker DJ, McPhee DA, Greenway AL, Ellett A, Chatfield C, Lawson VA, Crowe S, Maerz A, Sonza S, Learmont J, Sullivan JS, Cunningham A, Dwyer D, Dowton D, Mills J.** 1995. Genomic structure of an attenuated quasi species of HIV-1 from a blood transfusion donor and recipients. Science **270:**988–991. http://dx.doi.org/10.1126/science.270.5238.988.
2. **Kestler HW, Jeang KT.** 1995. Attenuated retrovirus vaccines and AIDS. Science **270:**1219–1222.
3. **Kirchhoff F, Greenough TC, Brettler DB, Sullivan JL, Desrosiers RC.** 1995. Brief report: absence of intact nef sequences in a long-term survivor with nonprogressive HIV-1 infection. N Engl J Med **332:**228–232. http://dx.doi.org/10.1056/NEJM199501263320405.
4. **Hanna Z, Kay DG, Rebai N, Guimond A, Jothy S, Jolicoeur P.** 1998. Nef harbors a major determinant of pathogenicity for an AIDS-like disease induced by HIV-1 in transgenic mice. Cell **95:**163–175. http://dx.doi.org/10.1016/S0092-8674(00)81748-1.
5. **Rahim MM, Chrobak P, Hu C, Hanna Z, Jolicoeur P.** 2009. Adult AIDS-like disease in a novel inducible human immunodeficiency virus type 1 Nef transgenic mouse model: CD4$^+$ T-cell activation is Nef dependent and can occur in the absence of lymphopenia. J Virol **83:**11830–11846. http://dx.doi.org/10.1128/JVI.01466-09.
6. **Garcia JV, Miller AD.** 1991. Serine phosphorylation-independent downregulation of cell-surface CD4 by *nef*. Nature **350:**508–511. http://dx.doi.org/10.1038/350508a0.
7. **Michel N, Allespach I, Venzke S, Fackler OT, Keppler OT.** 2005. The Nef protein of human immunodeficiency virus establishes superinfection immunity by a dual strategy to downregulate cell-surface CCR5 and CD4. Curr Biol **15:**714–723. http://dx.doi.org/10.1016/j.cub.2005.02.058.
8. **Collins KL, Chen BK, Kalams SA, Walker BD, Baltimore D.** 1998. HIV-1 Nef protein protects infected primary cells against killing by cytotoxic T lymphocytes. Nature **391:**397–401. http://dx.doi.org/10.1038/34929.
9. **Haller C, Müller B, Fritz JV, Lamas-Murua M, Stolp B, Pujol FM,**

Keppler OT, Fackler OT. 2014. HIV-1 Nef and Vpu are functionally redundant broad-spectrum modulators of cell surface receptors, including tetraspanins. J Virol **88:**14241–14257. http://dx.doi.org/10.1128/JVI.02333-14.

10. **Schwartz O, Maréchal V, Le Gall S, Lemonnier F, Heard JM.** 1996. Endocytosis of major histocompatibility complex class I molecules is induced by the HIV-1 Nef protein. Nat Med **2:**338–342. http://dx.doi.org/10.1038/nm0396-338.
11. **Aiken C, Trono D.** 1995. Nef stimulates human immunodeficiency virus type 1 proviral DNA synthesis. J Virol **69:**5048–5056.
12. **Chowers MY, Spina CA, Kwoh TJ, Fitch NJ, Richman DD, Guatelli JC.** 1994. Optimal infectivity in vitro of human immunodeficiency virus type 1 requires an intact *nef* gene. J Virol **68:**2906–2914.
13. **Pizzato M, Helander A, Popova E, Calistri A, Zamborlini A, Palù G, Göttlinger HG.** 2007. Dynamin 2 is required for the enhancement of HIV-1 infectivity by Nef. Proc Natl Acad Sci U S A **104:**6812–6817. http://dx.doi.org/10.1073/pnas.0607622104.
14. **Schwartz O, Maréchal V, Danos O, Heard JM.** 1995. Human immunodeficiency virus type 1 Nef increases the efficiency of reverse transcription in the infected cell. J Virol **69:**4053–4059.
15. **Fortin JF, Barat C, Beauséjour Y, Barbeau B, Tremblay MJ.** 2004. Hyper-responsiveness to stimulation of human immunodeficiency virus-infected $CD4^+$ T cells requires Nef and Tat virus gene products and results from higher NFAT, NF-kappaB, and AP-1 induction. J Biol Chem **279:**39520–39531. http://dx.doi.org/10.1074/jbc.M407477200.
16. **Pan X, Rudolph JM, Abraham L, Habermann A, Haller C, Krijnse-Locker J, Fackler OT.** 2012. HIV-1 Nef compensates for disorganization of the immunological synapse by inducing trans-Golgi network-associated Lck signaling. Blood **119:**786–797. http://dx.doi.org/10.1182/blood-2011-08-373209.
17. **Schindler M, Münch J, Kutsch O, Li H, Santiago ML, Bibollet-Ruche F, Müller-Trutwin MC, Novembre FJ, Peeters M, Courgnaud V, Bailes E, Roques P, Sodora DL, Silvestri G, Sharp PM, Hahn BH, Kirchhoff F.** 2006. Nef-mediated suppression of T cell activation was lost in a lentiviral lineage that gave rise to HIV-1. Cell **125:**1055–1067. http://dx.doi.org/10.1016/j.cell.2006.04.033.
18. **Schrager JA, Marsh JW.** 1999. HIV-1 Nef increases T cell activation in a stimulus-dependent manner. Proc Natl Acad Sci U S A **96:**8167–8172. http://dx.doi.org/10.1073/pnas.96.14.8167.
19. **Thoulouze MI, Sol-Foulon N, Blanchet F, Dautry-Varsat A, Schwartz O, Alcover A.** 2006. Human immunodeficiency virus type-1 infection impairs the formation of the immunological synapse. Immunity **24:**547–561. http://dx.doi.org/10.1016/j.immuni.2006.02.016.
20. **Sauter D, Hotter D, Van Driessche B, Stürzel CM, Kluge SF, Wildum S, Yu H, Baumann B, Wirth T, Plantier JC, Leoz M, Hahn BH, Van Lint C, Kirchhoff F.** 2015. Differential regulation of NF-kappaB-mediated proviral and antiviral host gene expression by primate lentiviral Nef and Vpu proteins. Cell Rep **10:**586–599. http://dx.doi.org/10.1016/j.celrep.2014.12.047.
21. **Arhel N, Lehmann M, Clauss K, Nienhaus GU, Piguet V, Kirchhoff F.** 2009. The inability to disrupt the immunological synapse between infected human T cells and APCs distinguishes HIV-1 from most other primate lentiviruses. J Clin Invest **119:**2965–2975. http://dx.doi.org/10.1172/JCI38994.
22. **Haller C, Rauch S, Fackler OT.** 2007. HIV-1 Nef employs two distinct mechanisms to modulate Lck subcellular localization and TCR induced actin remodeling. PLoS One **2:**e1212. http://dx.doi.org/10.1371/journal.pone.0001212.
23. **Haller C, Rauch S, Michel N, Hannemann S, Lehmann MJ, Keppler OT, Fackler OT.** 2006. The HIV-1 pathogenicity factor Nef interferes with maturation of stimulatory T-lymphocyte contacts by modulation of N-Wasp activity. J Biol Chem **281:**19618–19630. http://dx.doi.org/10.1074/jbc.M513802200.
24. **Pan X, Geist MM, Rudolph JM, Nickel W, Fackler OT.** 2013. HIV-1 Nef disrupts membrane-microdomain-associated anterograde transport for plasma membrane delivery of selected Src family kinases. Cell Microbiol **15:**1605–1621. http://dx.doi.org/10.1111/cmi.12148.
25. **Rudolph JM, Eickel N, Haller C, Schindler M, Fackler OT.** 2009. Inhibition of T-cell receptor-induced action remodeling and relocalization of Lck are evolutionarily conserved activities of lentiviral Nef proteins. J Virol **83:**11528–11539. http://dx.doi.org/10.1128/JVI.01423-09.
26. **Abraham L, Bankhead P, Pan X, Engel U, Fackler OT.** 2012. HIV-1 Nef limits communication between linker of activated T cells and SLP-76 to reduce formation of SLP-76-signaling microclusters following TCR stimulation. J Immunol **189:**1898–1910. http://dx.doi.org/10.4049/jimmunol.1200652.
27. **Abraham L, Fackler OT.** 2012. HIV-1 Nef: a multifaceted modulator of T cell receptor signaling. Cell Commun Signal **10:**39. http://dx.doi.org/10.1186/1478-811X-10-39.
28. **Fackler OT, Luo W, Geyer M, Alberts AS, Peterlin BM.** 1999. Activation of Vav by Nef induces cytoskeletal rearrangements and downstream effector functions. Mol Cell **3:**729–739. http://dx.doi.org/10.1016/S1097-2765(01)80005-8.
29. **Nobile C, Rudnicka D, Hasan M, Aulner N, Porrot F, Machu C, Renaud O, Prévost MC, Hivroz C, Schwartz O, Sol-Foulon N.** 2010. HIV-1 Nef inhibits ruffles, induces filopodia, and modulates migration of infected lymphocytes. J Virol **84:**2282–2293. http://dx.doi.org/10.1128/JVI.02230-09.
30. **Stolp B, Imle A, Coelho FM, Hons M, Gorina R, Lyck R, Stein JV, Fackler OT.** 2012. HIV-1 Nef interferes with T-lymphocyte circulation through confined environments in vivo. Proc Natl Acad Sci U S A **109:**18541–18546. http://dx.doi.org/10.1073/pnas.1204322109.
31. **Stolp B, Reichman-Fried M, Abraham L, Pan X, Giese SI, Hannemann S, Goulimari P, Raz E, Grosse R, Fackler OT.** 2009. HIV-1 Nef interferes with host cell motility by deregulation of cofilin. Cell Host Microbe **6:**174–186. http://dx.doi.org/10.1016/j.chom.2009.06.004.
32. **Lu TC, He JC, Wang ZH, Feng X, Fukumi-Tominaga T, Chen N, Xu J, Iyengar R, Klotman PE.** 2008. HIV-1 Nef disrupts the podocyte actin cytoskeleton by interacting with diaphanous interacting protein. J Biol Chem **283:**8173–8182. http://dx.doi.org/10.1074/jbc.M708920200.
33. **Choe EY, Schoenberger ES, Groopman JE, Park IW.** 2002. HIV Nef inhibits T cell migration. J Biol Chem **277:**46079–46084. http://dx.doi.org/10.1074/jbc.M204698200.
34. **Janardhan A, Swigut T, Hill B, Myers MP, Skowronski J.** 2004. HIV-1 Nef binds the DOCK2-ELMO1 complex to activate Rac and inhibit lymphocyte chemotaxis. PLoS Biol **2:**E6. http://dx.doi.org/10.1371/journal.pbio.0020006.
35. **Stolp B, Abraham L, Rudolph JM, Fackler OT.** 2010. Lentiviral Nef proteins utilize PAK2-mediated deregulation of cofilin as a general strategy to interfere with actin remodeling. J Virol **84:**3935–3948. http://dx.doi.org/10.1128/JVI.02467-09.
36. **Fackler OT, Murooka TT, Imle A, Mempel TR.** 2014. Adding new dimensions: towards an integrative understanding of HIV-1 spread. Nat Rev Microbiol **12:**563–574. http://dx.doi.org/10.1038/nrmicro3309.
37. **Geyer M, Fackler OT, Peterlin BM.** 2001. Structure-function relationships in HIV-1 Nef. EMBO Rep **2:**580–585. http://dx.doi.org/10.1093/embo-reports/kve141.
38. **Saksela K.** 2011. Interactions of the HIV/SIV pathogenicity factor Nef with SH3 domain-containing host cell proteins. Curr HIV Res **9:**531–542. http://dx.doi.org/10.2174/157016211798842107.
39. **Laguette N, Brégnard C, Benichou S, Basmaciogullari S.** 2010. Human immunodeficiency virus (HIV) type-1, HIV-2 and simian immunodeficiency virus Nef proteins. Mol Aspects Med **31:**418–433. http://dx.doi.org/10.1016/j.mam.2010.05.003.
40. **Agopian K, Wei BL, Garcia JV, Gabuzda D.** 2006. A hydrophobic binding surface on the human immunodeficiency virus type 1 Nef core is critical for association with p21-activated kinase 2. J Virol **80:**3050–3061. http://dx.doi.org/10.1128/JVI.80.6.3050-3061.2006.
41. **O'Neill E, Kuo LS, Krisko JF, Tomchick DR, Garcia JV, Foster JL.** 2006. Dynamic evolution of the human immunodeficiency virus type 1 pathogenic factor, Nef. J Virol **80:**1311–1320. http://dx.doi.org/10.1128/JVI.80.3.1311-1320.2006.
42. **Schindler M, Rajan D, Specht A, Ritter C, Pulkkinen K, Saksela K, Kirchhoff F.** 2007. Association of Nef with p21-activated kinase 2 is dispensable for efficient human immunodeficiency virus type 1 replication and cytopathicity in ex vivo-infected human lymphoid tissue. J Virol **81:**13005–13014. http://dx.doi.org/10.1128/JVI.01436-07.
43. **Renkema GH, Manninen A, Mann DA, Harris M, Saksela K.** 1999. Identification of the Nef-associated kinase as p21-activated kinase 2. Curr Biol **9:**1407–1410. http://dx.doi.org/10.1016/S0960-9822(00)80086-X.
44. **Renkema GH, Manninen A, Saksela K.** 2001. Human immunodeficiency virus type 1 Nef selectively associates with a catalytically active subpopulation of p21-activated kinase 2 (PAK2) independently of PAK2 binding to Nck or beta-PIX. J Virol **75:**2154–2160. http://dx.doi.org/10.1128/JVI.75.5.2154-2160.2001.
45. **Kuo LS, Baugh LL, Denial SJ, Watkins RL, Liu M, Garcia JV, Foster JL.**

2012. Overlapping effector interfaces define the multiple functions of the HIV-1 Nef polyproline helix. Retrovirology **9**:47. http://dx.doi.org/10.1186/1742-4690-9-47.

46. **Stolp B, Fackler OT**. 2011. How HIV takes advantage of the cytoskeleton in entry and replication. Viruses **3**:293–311. http://dx.doi.org/10.3390/v3040293.
47. **Krautkrämer E, Giese SI, Gasteier JE, Muranyi W, Fackler OT**. 2004. Human immunodeficiency virus type 1 Nef activates p21-activated kinase via recruitment into lipid rafts. J Virol **78**:4085–4097. http://dx.doi.org/10.1128/JVI.78.8.4085-4097.2004.
48. **Pulkkinen K, Renkema GH, Kirchhoff F, Saksela K**. 2004. Nef associates with p21-activated kinase 2 in a p21-GTPase-dependent dynamic activation complex within lipid rafts. J Virol **78**:12773–12780. http://dx.doi.org/10.1128/JVI.78.23.12773-12780.2004.
49. **Fackler OT, Lu X, Frost JA, Geyer M, Jiang B, Luo W, Abo A, Alberts AS, Peterlin BM**. 2000. p21-activated kinase 1 plays a critical role in cellular activation by Nef. Mol Cell Biol **20**:2619–2627. http://dx.doi.org/10.1128/MCB.20.7.2619-2627.2000.
50. **Nunn MF, Marsh JW**. 1996. Human immunodeficiency virus type 1 Nef associates with a member of the p21-activated kinase family. J Virol **70**:6157–6161.
51. **Rauch S, Pulkkinen K, Saksela K, Fackler OT**. 2008. Human immunodeficiency virus type 1 Nef recruits the guanine exchange factor Vav1 via an unexpected interface into plasma membrane microdomains for association with p21-activated kinase 2 activity. J Virol **82**:2918–2929. http://dx.doi.org/10.1128/JVI.02185-07.
52. **Renkema GH, Pulkkinen K, Saksela K**. 2002. Cdc42/Rac1-mediated activation primes PAK2 for superactivation by tyrosine phosphorylation. Mol Cell Biol **22**:6719–6725. http://dx.doi.org/10.1128/MCB.22.19.6719-6725.2002.
53. **Mukerji J, Olivieri KC, Misra V, Agopian KA, Gabuzda D**. 2012. Proteomic analysis of HIV-1 Nef cellular binding partners reveals a role for exocyst complex proteins in mediating enhancement of intercellular nanotube formation. Retrovirology **9**:33. http://dx.doi.org/10.1186/1742-4690-9-33.
54. **Jäger S, Cimermancic P, Gulbahce N, Johnson JR, McGovern KE, Clarke SC, Shales M, Mercenne G, Pache L, Li K, Hernandez H, Jang GM, Roth SL, Akiva E, Marlett J, Stephens M, D'Orso I, Fernandes J, Fahey M, Mahon C, O'Donoghue AJ, Todorovic A, Morris JH, Maltby DA, Alber T, Cagney G, Bushman FD, Young JA, Chanda SK, Sundquist WI, Kortemme T, Hernandez RD, Craik CS, Burlingame A, Sali A, Frankel AD, Krogan NJ**. 2012. Global landscape of HIV-human protein complexes. Nature **481**:365–370. http://dx.doi.org/10.1038/nature10719.
55. **Mohammadi S, Isberg RR**. 2013. Cdc42 interacts with the exocyst complex to promote phagocytosis. J Cell Biol **200**:81–93. http://dx.doi.org/10.1083/jcb.201204090.
56. **Sakurai-Yageta M, Recchi C, Le Dez G, Sibarita JB, Daviet L, Camonis J, D'Souza-Schorey C, Chavrier P**. 2008. The interaction of IQGAP1 with the exocyst complex is required for tumor cell invasion downstream of Cdc42 and RhoA. J Cell Biol **181**:985–998. http://dx.doi.org/10.1083/jcb.200709076.
57. **Moskalenko S, Henry DO, Rosse C, Mirey G, Camonis JH, White MA**. 2002. The exocyst is a Ral effector complex. Nat Cell Biol **4**:66–72. http://dx.doi.org/10.1038/ncb728.
58. **Moskalenko S, Tong C, Rosse C, Mirey G, Formstecher E, Daviet L, Camonis J, White MA**. 2003. Ral GTPases regulate exocyst assembly through dual subunit interactions. J Biol Chem **278**:51743–51748. http://dx.doi.org/10.1074/jbc.M308702200.
59. **Sugihara K, Asano S, Tanaka K, Iwamatsu A, Okawa K, Ohta Y**. 2002. The exocyst complex binds the small GTPase RalA to mediate filopodia formation. Nat Cell Biol **4**:73–78. http://dx.doi.org/10.1038/ncb720.
60. **Zhao Y, Liu J, Yang C, Capraro BR, Baumgart T, Bradley RP, Ramakrishnan N, Xu X, Radhakrishnan R, Svitkina T, Guo W**. 2013. Exo70 generates membrane curvature for morphogenesis and cell migration. Dev Cell **26**:266–278. http://dx.doi.org/10.1016/j.devcel.2013.07.007.
61. **Zuo X, Zhang J, Zhang Y, Hsu SC, Zhou D, Guo W**. 2006. Exo70 interacts with the Arp2/3 complex and regulates cell migration. Nat Cell Biol **8**:1383–1388. http://dx.doi.org/10.1038/ncb1505.
62. **Hase K, Kimura S, Takatsu H, Ohmae M, Kawano S, Kitamura H, Ito M, Watarai H, Hazelett CC, Yeaman C, Ohno H**. 2009. M-Sec promotes membrane nanotube formation by interacting with Ral and the exocyst complex. Nat Cell Biol **11**:1427–1432. http://dx.doi.org/10.1038/ncb1990.
63. **Baust T, Czupalla C, Krause E, Bourel-Bonnet L, Hoflack B**. 2006. Proteomic analysis of adaptor protein 1A coats selectively assembled on liposomes. Proc Natl Acad Sci U S A **103**:3159–3164. http://dx.doi.org/10.1073/pnas.0511062103.
64. **Rivera-Molina F, Toomre D**. 2013. Live-cell imaging of exocyst links its spatiotemporal dynamics to various stages of vesicle fusion. J Cell Biol **201**:673–680. http://dx.doi.org/10.1083/jcb.201212103.
65. **Piguet V, Wan L, Borel C, Mangasarian A, Demaurex N, Thomas G, Trono D**. 2000. HIV-1 Nef protein binds to the cellular protein PACS-1 to downregulate class I major histocompatibility complexes. Nat Cell Biol **2**:163–167. http://dx.doi.org/10.1038/35004038.
66. **Atkins KM, Thomas L, Youker RT, Harriff MJ, Pissani F, You H, Thomas G**. 2008. HIV-1 Nef binds PACS-2 to assemble a multikinase cascade that triggers major histocompatibility complex class I (MHC-I) down-regulation: analysis using short interfering RNA and knock-out mice. J Biol Chem **283**:11772–11784. http://dx.doi.org/10.1074/jbc.M707572200.
67. **Baugh LL, Garcia JV, Foster JL**. 2008. Functional characterization of the human immunodeficiency virus type 1 Nef acidic domain. J Virol **82**:9657–9667. http://dx.doi.org/10.1128/JVI.00107-08.
68. **Giese SI, Woerz I, Homann S, Tibroni N, Geyer M, Fackler OT**. 2006. Specific and distinct determinants mediate membrane binding and lipid raft incorporation of HIV-1(SF2) Nef. Virology **355**:175–191. http://dx.doi.org/10.1016/j.virol.2006.07.003.
69. **Craig HM, Pandori MW, Guatelli JC**. 1998. Interaction of HIV-1 Nef with the cellular dileucine-based sorting pathway is required for CD4 down-regulation and optimal viral infectivity. Proc Natl Acad Sci U S A **95**:11229–11234. http://dx.doi.org/10.1073/pnas.95.19.11229.
70. **Lu X, Yu H, Liu SH, Brodsky FM, Peterlin BM**. 1998. Interactions between HIV1 Nef and vacuolar ATPase facilitate the internalization of CD4. Immunity **8**:647–656. http://dx.doi.org/10.1016/S1074-7613(00)80569-5.
71. **Baur AS, Sass G, Laffert B, Willbold D, Cheng-Mayer C, Peterlin BM**. 1997. The N-terminus of Nef from HIV-1/SIV associates with a protein complex containing Lck and a serine kinase. Immunity **6**:283–291. http://dx.doi.org/10.1016/S1074-7613(00)80331-3.
72. **Fackler OT, Wolf D, Weber HO, Laffert B, D'Aloja P, Schuler-Thurner B, Geffin R, Saksela K, Geyer M, Peterlin BM, Schuler G, Baur AS**. 2001. A natural variability in the proline-rich motif of Nef modulates HIV-1 replication in primary T cells. Curr Biol **11**:1294–1299. http://dx.doi.org/10.1016/S0960-9822(01)00373-6.
73. **Parrini MC, Lei M, Harrison SC, Mayer BJ**. 2002. Pak1 kinase homodimers are autoinhibited in *trans* and dissociated upon activation by Cdc42 and Rac1. Mol Cell **9**:73–83. http://dx.doi.org/10.1016/S1097-2765(01)00428-2.
74. **Mangasarian A, Piguet V, Wang JK, Chen YL, Trono D**. 1999. Nef-induced CD4 and major histocompatibility complex class I (MHC-I) down-regulation are governed by distinct determinants: N-terminal alpha helix and proline repeat of Nef selectively regulate MHC-I trafficking. J Virol **73**:1964–1973.
75. **Geist MM, Pan X, Bender S, Bartenschlager R, Nickel W, Fackler OT**. 2014. Heterologous Src homology 4 domains support membrane anchoring and biological activity of HIV-1 Nef. J Biol Chem **289**:14030–14044. http://dx.doi.org/10.1074/jbc.M114.563528.
76. **Dustin ML, Chakraborty AK, Shaw AS**. 2010. Understanding the structure and function of the immunological synapse. Cold Spring Harb Perspect Biol **2**:a002311. http://dx.doi.org/10.1101/cshperspect.a002311.
77. **Billadeau DD, Nolz JC, Gomez TS**. 2007. Regulation of T-cell activation by the cytoskeleton. Nat Rev Immunol **7**:131–143. http://dx.doi.org/10.1038/nri2021.
78. **Lee JH, Wittki S, Bräu T, Dreyer FS, Krätzel K, Dindorf J, Johnston IC, Gross S, Kremmer E, Zeidler R, Schlötzer-Schrehardt U, Lichtenheld M, Saksela K, Harrer T, Schuler G, Federico M, Baur AS**. 2013. HIV Nef, paxillin, and Pak1/2 regulate activation and secretion of TACE/ADAM10 proteases. Mol Cell **49**:668–679. http://dx.doi.org/10.1016/j.molcel.2012.12.004.
79. **TerBush DR, Maurice T, Roth D, Novick P**. 1996. The exocyst is a multiprotein complex required for exocytosis in Saccharomyces cerevisiae. EMBO J **15**:6483–6494.
80. **Muratori C, Cavallin LE, Krätzel K, Tinari A, De Milito A, Fais S, D'Aloja P, Federico M, Vullo V, Fomina A, Mesri EA, Superti F, Baur**

AS. 2009. Massive secretion by T cells is caused by HIV Nef in infected cells and by Nef transfer to bystander cells. Cell Host Microbe **6:**218–230. http://dx.doi.org/10.1016/j.chom.2009.06.009.

81. **Lenassi M, Cagney G, Liao M, Vaupotic T, Bartholomeeusen K, Cheng Y, Krogan NJ, Plemenitas A, Peterlin BM**. 2010. HIV Nef is secreted in exosomes and triggers apoptosis in bystander $CD4^-$ T cells. Traffic **11:** 110–122. http://dx.doi.org/10.1111/j.1600-0854.2009.01006.x.
82. **Arenaccio C, Chiozzini C, Columba-Cabezas S, Manfredi F, Affabris E, Baur A, Federico M**. 2014. Exosomes from human immunodeficiency virus type 1 (HIV-1)-infected cells license quiescent $CD4^+$ T lymphocytes to replicate HIV-1 through a Nef- and ADAM17-dependent mechanism. J Virol **88:**11529–11539. http://dx.doi.org/10.1128/JVI.01712-14.
83. **Smithgall TE, Thomas G**. 2013. Small molecule inhibitors of the HIV-1 virulence factor, Nef. Drug Discov Today Technol **10:**e523–e529. http://dx.doi.org/10.1016/j.ddtec.2013.07.002.
84. **Trible RP, Narute P, Emert-Sedlak LA, Alvarado JJ, Atkins K, Thomas L, Kodama T, Yanamala N, Korotchenko V, Day BW, Thomas G, Smithgall TE**. 2013. Discovery of a diaminoquinoxaline benzenesulfonamide antagonist of HIV-1 Nef function using a yeast-based phenotypic screen. Retrovirology **10:**135. http://dx.doi.org/10.1186/1742-4690-10-135.
85. **Dikeakos JD, Atkins KM, Thomas L, Emert-Sedlak L, Byeon IJ, Jung J, Ahn J, Wortman MD, Kukull B, Saito M, Koizumi H, Williamson DM, Hiyoshi M, Barklis E, Takiguchi M, Suzu S, Gronenborn AM, Smithgall TE, Thomas G**. 2010. Small molecule inhibition of HIV-1-induced MHC-I down-regulation identifies a temporally regulated switch in Nef action. Mol Biol Cell **21:**3279–3292. http://dx.doi.org/10.1091/mbc.E10-05-0470.
86. **Rane CK, Minden A**. 2014. P21 activated kinases: structure, regulation, and functions. Small GTPases **5:**e28003. http://dx.doi.org/10.4161/sgtp.28003.
87. **Radu M, Semenova G, Kosoff R, Chernoff J**. 2014. PAK signalling during the development and progression of cancer. Nat Rev Cancer **14:**13–25. http://dx.doi.org/10.1038/nrc3645.